The Astrophysical Journal, 991:6 (10pp), 2025 September 20 https://doi.org/10.3847/1538-4357/adf8e8

Reprocessing of the Parkes 70 cm Survey and Discovery of a New Radio Pulsar in the Large Magellanic Cloud

Wenke Xia[1,2,3], Fronefield Crawford[1], Shinnosuke Hisano[4], Tai Jespersen[1], Melanie Ficarra[1], Mckenzie Golden[1], and Mia Gironda[1]

[1] Department of Physics and Astronomy, Franklin and Marshall College, P.O. Box 3003, Lancaster, PA 17604, USA; wenke.xia@mail.mcgill.ca
[2] Department of Physics, McGill University, 3600 rue University, Montreal, QC H3A 2T8, Canada
[3] Trottier Space Institute, McGill University, 3550 rue University, Montreal, QC H3A 2A7, Canada
[4] Kumamoto University, Graduate School of Science and Technology, Kumamoto, 860-8555, Japan
Received 2025 February 20; revised 2025 July 28; accepted 2025 July 28; published 2025 September 11

Abstract

We have reprocessed the data archived from the Parkes 70 cm (PKS70) pulsar survey with an expanded dispersion measure (DM) search range and an acceleration search. Our goal was to detect pulsars that might have been missed in the original survey processing. Of the original 43,842 pointings, 34,869 pointings were archived, along with 440 additional pointings for confirmation or timing. We processed all of these archived data and detected 359 known pulsars: 265 of these were detected in the original survey, while an additional 94 currently known pulsars were detected in our reprocessing. A few among those 94 pulsars are highly accelerated binary pulsars. Furthermore, we detected 5 more pulsars with DMs higher than the original survey thresholds, as well as 6 more pulsars below the nominal survey sensitivity threshold (from the original survey beams with longer integrations). We missed detection of 33 (of the 298) pulsars detected in the original survey, in part because of portions of the survey data missing in the archive and our early-stage candidate sifting method. We discovered one new pulsar in the reanalysis, PSR J0540−69, which has a spin period of 0.909 s and resides in the Large Magellanic Cloud (LMC). This new pulsar appeared in three PKS70 beams and one additional *L*-band observation that targeted the LMC pulsar PSR B0540−69. The numerous pulsar detections found in our reanalysis and the discovery of a new pulsar in the LMC highlight the value of conducting multiple searches through pulsar data sets.

Unified Astronomy Thesaurus concepts: Surveys (1671); Radio pulsars (1353)

Materials only available in the online version of record: data behind figure

1. Introduction and Motivation

1.1. PKS70 Survey and Data Archive

The Parkes 70 cm (PKS70) pulsar survey was conducted at the 64 m Parkes telescope ("Murriyang") in the 1990s, covering the southern sky visible from the telescope. The survey observations were centered at 436 MHz with a bandwidth of 32 MHz split into 256 channels. The data were sampled at 0.3 ms, making the survey not very sensitive to millisecond pulsars (MSPs). Typical integrations were 157 s per pointing, and the limiting flux density in the original survey was about 3 mJy (but falls off significantly for MSPs and at low Galactic latitudes; see Figure 6 of R. N. Manchester et al. 1996). These observing parameters are listed in Table 1.

In the original survey publications (R. N. Manchester et al. 1996; N. D'Amico et al. 1998; A. G. Lyne et al. 1998), the authors reported observing and searching 43,842 tiled, blind survey beams out of the total originally planned gridded survey area of 44,299 beams that were to cover the southern sky. A total of 298 pulsars were detected, including 101 new pulsars and 197 pulsars that were known at the time.

Of these gridded survey observations, 41,342 were archived, pointing at 34,869 different positions. The remainder of the data was likely lost or was stored on damaged tapes, but its fate is uncertain (D. Lorimer 2025, private communication). A small fraction (2%) of the gridded observations had an integration time that was noticeably longer than the nominal integration of 157 s. The cause could be that the original survey observed some positions with different integrations, or it could be because these were makeup observations of corrupted or bad observations. In addition to these gridded survey beams, 1774 observations with 440 different targeted positions (some of which were the same as the gridded positions, most likely candidate confirmation beams or timing observations) were recorded as part of the survey and were archived in the project. These additional targeted beams are mostly recorded at 436 (86% of the targeted beams, with 0.125 MHz channel width) and 1400 MHz (14% of the targeted beams, with 2–5 MHz channel width). Their integration time ranged from a few seconds (likely test observations or corrupted data) to ∼12 hr, targeting the Small Magellanic Cloud (SMC) and Large Magellanic Cloud (LMC); despite the large range, most observations were 5–10 minutes. With the original survey and additional observations, the complete archive contained 43,116 observations (35,279 pointing positions, representing 80% of the original pointing positions) available for reprocessing.

Figure 1 shows the sky coverage of the full archival survey beams in gray. Note that this does not include the missing 20% of the survey that was not archived, which mainly corresponds to the white patches within the survey region. The additional beams are also shown in blue dots; some of these lie outside of the nominal survey region, while many lie within that region without following the pattern of the survey beam map.

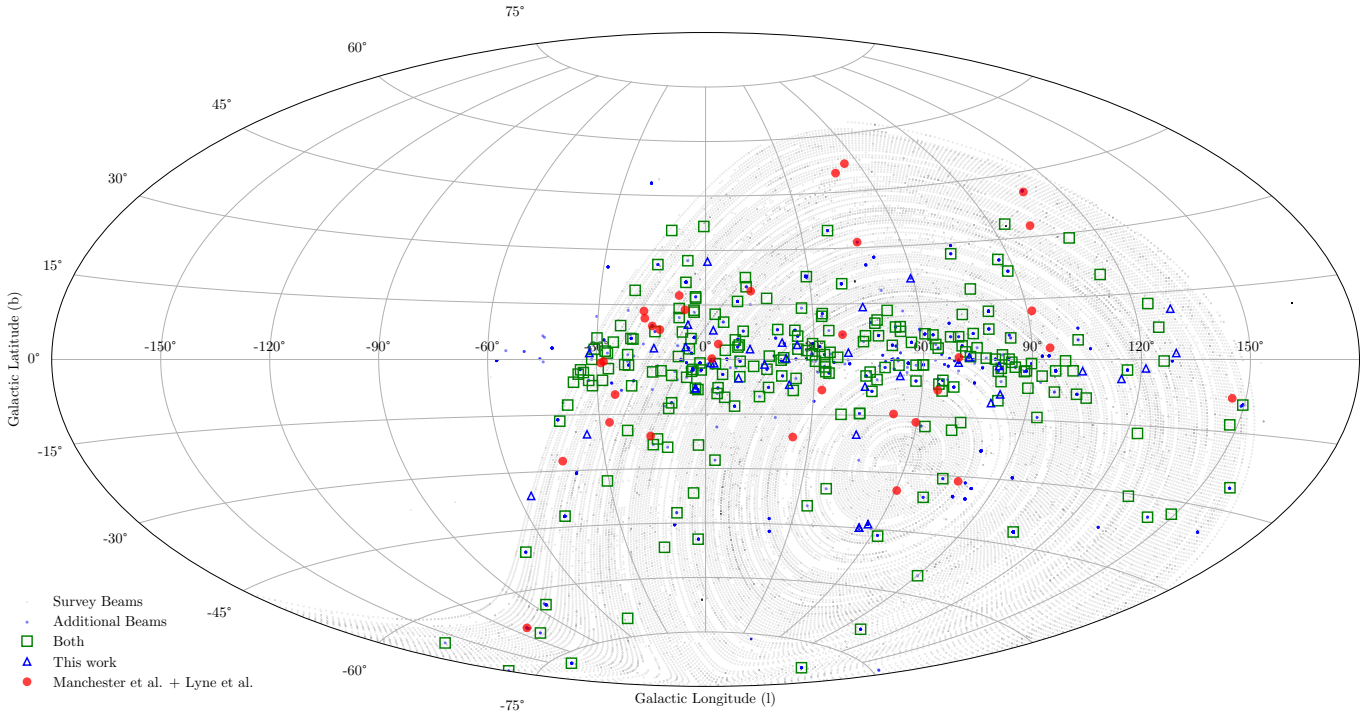

Figure 1. Sky plot of the PKS70 survey beam coverage from archival survey beams (small gray circles) and additional observations (small blue circles), shown in Galactic coordinates. The white patches in the sky coverage indicate where the survey beam data are missing in the archive. Pulsars detected by both the original survey and our reprocessing are shown as green squares, while pulsars detected only in our reprocessing are shown as blue triangles. Pulsars detected in the original processing but not in our reprocessing are plotted as red circles.

1.2. New Processing of the Survey Archive

We downloaded raw data from the CSIRO Data Archive[5] and reprocessed the entire survey archive to search for previously missed pulsars and fast radio bursts (FRBs). A search for single pulses and FRBs in the survey data had not been conducted previously. We completed this search prior to the periodicity search described here. The search resulted in the discovery of four new, long-duration (>50 ms) FRBs, which were reported by F. Crawford et al. (2022).

The reprocessing described here for new periodic pulsar signals is motivated by two factors. The first is that the newer software we are using for the periodicity search (PRESTO; S. M. Ransom 2001; S. M. Ransom et al. 2002) was not available at the time of the original survey. This has better radio frequency interference (RFI) excision and visualization features than the older software used in the original data processing. Thus, there may be pulsars in the data that were missed. The second is that, with the vastly increased computational power available now compared to what was available at the time of the original survey, we can explore an expanded search parameter space within a reasonable amount of computational time. We searched up to a much larger maximum DM (3000 pc cm^{-3}, compared with the maximum DM of 777 pc cm^{-3} in the original processing), which could reveal unexpectedly high-DM pulsars in the data. We also used PRESTO's built-in dedispersion, a modern dedispersion algorithm in contrast to the algorithm from the origin survey that used a linear approximation in the first stage of dedispersion (R. N. Manchester et al. 1996; A. G. Lyne et al. 1998; J. H. Taylor 1974). The newer dedispersion algorithm is more computationally intensive but results in improved sensitivity at higher DMs, as it avoids the additional smearing effect caused by the approximation. Lastly, the increased computational power allowed us to conduct a search for accelerated (binary) pulsars, which was not done in the original processing. This allowed us to maintain sensitivity to even highly accelerated binary systems, which could have been missed in the prior analysis. Such systems are rare but important to study, as they are ideal systems for testing theories of gravity and gravitational waves (J. H. Taylor & J. M. Weisberg 1989; J. M. Weisberg & J. H. Taylor 2003, 2005).

In this paper, we report on our analysis of the survey data, discuss both the pulsar redetections and those that were missed, and report on the discovery of a new pulsar in the LMC, PSR J0540−69, which appeared in three targeted observations of the X-ray pulsar PSR B0540−69 (F. D. Seward et al. 1984) in the PKS70 survey archive and one other nonsurvey *L*-band LMC observation.

2. Search Methods and Analysis

We processed all the archived data available from the PK70 archive, including both gridded and targeted beams. We first searched each beam for RFI and masked it prior to analysis using the rfifind script in PRESTO. A time window of 1 s was specified, while the default values were used for the rest of the parameters. The mean (and median) fraction of data flagged and masked as RFI for the analyzed files was 10%, but this ranged widely across the data set (from 0% to 99.96%). Only 205 (about half a percent) of the collection of beams had RFI flagging of more than 50%. Of these 205, all but 29 were reobserved successfully.

We then dedispersed each beam into 1453 separate DM steps between 0 and 3000 pc cm^{-3} in several stages. The DM spacing, downsampling, and range of DMs used in each stage

[5] https://data.csiro.au

Table 1
PKS70 Survey Parameters

Parameter	Value
Central observing frequency (MHz)	436
Bandwidth (MHz)	32
Number of channels	256
Sampling time (μs)	300
Integration time per pointing (s)	157.3
Gain	0.64 K Jy^{-1}
System temperature	$\sim$50 $_{\text{(receiver)}}$ + 25 $_{\text{(sky)}}$

Note. See R. N. Manchester et al. (1996).

were obtained by using the DDPlan.py script in PRESTO (see Table 2). This DM range is significantly larger than the prior search and goes beyond the Galactic electron layer in all directions (J. M. Cordes & T. J. W. Lazio 2002). In contrast, to reduce processing time, the previous search dedispersed the data with a direction-dependent maximum DM, which was the smaller of 777 pc cm^{-3} and $42/\sin b$ pc cm^{-3}, where b is the Galactic latitude (R. N. Manchester et al. 1996). The greater DM range in this reprocessing allowed for the detection of pulsars with DMs larger than the expected maximum DM value in case of local regions of plasma between us and the pulsar (see Figure 2).

Each dedispersed time series was high-pass filtered and searched for periodicities with an acceleration range that corrected for a Fourier power spectrum bin drift of 50 bins over the course of the integration. The maximum acceleration to which this corresponds is $a_{\max} = z_{\max} cP/hT^2$, where $z_{\max}$ is 50, the maximum bin drift, h is 8, the number of harmonics used in the search, T is 157 s (the typical integration time per beam; see Table 1), c is the speed of light, and P is the pulsar's spin period. We used the native 0.3 ms sampling in the search, which maintained good sensitivity to pulsars with spin periods greater than about 3 ms for DMs $\lesssim$100 pc cm^{-3} (see Figure 3). Our search maintained full sensitivity to pulsars with a maximum acceleration of 230 m s^{-2} (for a 3 ms spin period), making this search sensitive to highly accelerated binaries (see Figure 4). Note that the pulsar with the highest currently known acceleration, the double neutron star PSR J1757−1854 (A. D. Cameron et al. 2018), with a spin period of 21.5 ms, has a maximum periastron acceleration of 684 m s^{-2} and is within the range where it would have been detectable in our acceleration search (although its flux density is too low for detection in this survey by at least 1 order of magnitude). The periodicity candidates identified from the search were then collected and sifted. The sifting process involved removing redundant candidates in each beam, based on their periods and DMs. Only the candidate with the strongest signal-to-noise ratio (S/N) in the redundancies was retained. In addition, any candidates appearing in fewer than 10 DM trials or with a spin period less than 3 ms were removed in order to reduce the total number of final candidates to investigate further. Note that this period restriction prevented us from detecting pulsars having periods less than 3 ms in the blind search. The period and DM for each candidate were used to refold the data at periods and DMs near these nominal values using the prepfold package in PRESTO.

Our reprocessing resulted in a total of 364,087 candidates. To inspect such a large number of candidates, we developed a web-based plot visualization and rating tool for displaying

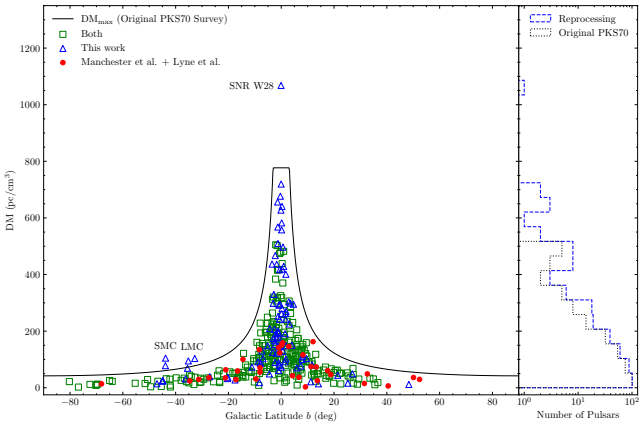

Figure 2. DMs of detected pulsars in both the original survey and this new reprocessing. The left panel shows the DM vs. Galactic latitude b of known pulsars detected in the original survey (red circles and green squares) and in this new reprocessing (blue triangles and green squares), along with the maximum DM searched in the original survey (black line). With a higher maximum DM (up to 3000 pc cm^{-3}), five additional known pulsars with excessive DMs were detected in this reprocessing. The excess DM of all five pulsars is attributed to their local environments—four are located in the SMC or LMC, and one is associated with a known supernova remnant, as noted in the figure. The right panel shows the distribution of the DMs of all the pulsars detected in the original PKS70 survey (black) and in this reprocessing (blue). The DM distribution of pulsars detected in the reprocessing expands into higher DM values compared to the original survey.
(The data used to create this figure are available in the online article.)

Table 2
Dedispersion Plan for Survey Search

DM Range	DM Step	Number of DM Trials	Downsampling
0.0–85.0	0.2	425	1
85.0–132.1	0.3	157	2
132.1–198.6	0.5	133	3
198.6–354.6	1.0	156	5
354.6–463.6	1.0	109	8
463.6–773.6	2.0	155	12
773.6–1723.6	5.0	190	24
1723.6–3003.6	10.0	128	48

Note. Parameters obtained from the DDplan.py script in PRESTO. All DM values are in pc cm^{-3}.

candidate plots and cataloging classifications from these plots. Teams of undergraduate students from several institutions that are part of the NANOGrav Physics Frontiers Center[6] were engaged in classifying the candidates. A total of 64 students from nine institutions rated these plots. To identify known pulsars, we used Pulsar Scraper[7] (D. L. Kaplan 2022) to search for coincident periods (or harmonics of periods), DMs, and coordinates within the Parkes beam size. Candidates with corresponding entries were classified as detections of known pulsars.

3. Results and Discussion

We blindly detected 359 known pulsars in our processing, where 256 pulsars were from gridded beams and 103 pulsars were from targeted beams, and further details are provided in Tables 3 and 4. The original survey indicated that all 298

[6] https://nanograv.org
[7] https://pulsar.cgca-hub.org/search

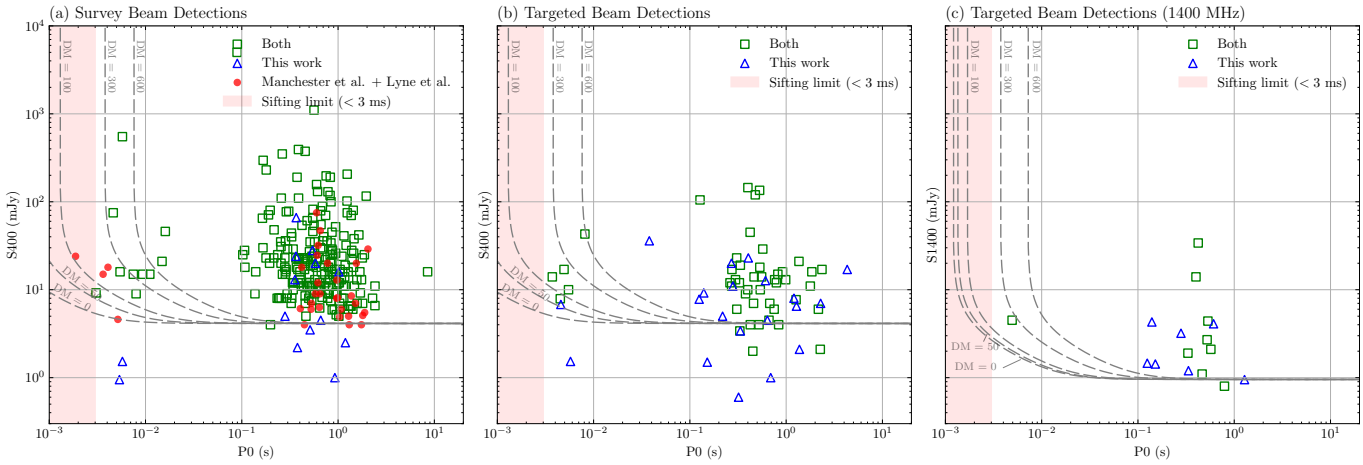

Figure 3. Flux density vs. spin period of known pulsars in the region observed; pulsars detected from at least one survey beam are shown in panel (a), and the pulsars detected only from targeted beams are shown in panel (b) and (c). In panel (a), sensitivity curves are shown for representative DMs (0, 50, 100, 300, and 500 pc cm^{-3}) and are assuming a duty cycle of 0.08, a detection S/N of 8, and a digitization loss constant β of 1.5 in the radiometer equation (R. N. Manchester et al. 1996; A. G. Lyne et al. 1998). They also include the effects of dispersive smearing within channels and the sampling time (but not the effects of interstellar scattering), which degrade the sensitivity at small periods. Several pulsars (blue triangles) were detected in our reanalysis that have flux densities below the nominal survey limit, including two with spin periods of less than 10 ms. These detections were made from observations with longer integrations. In panel (b), the same curves are plotted along with known pulsars that were detected only in an additional targeted beam. Some pulsars are only detected in a targeted beam centered at higher frequencies (*L*-band) and are plotted in panel (c). We also estimated the sensitivity curves for *L*-band detections using a sampling time of 1.2 ms, a central frequency of 1400 MHz with 5 MHz resolution, and a typical integration time of 300 s. The remaining assumptions are the same as those in the calculation at 400 MHz. Our candidate sifting process removed candidates with periods under 3 ms, and this range is shown by the shaded region.

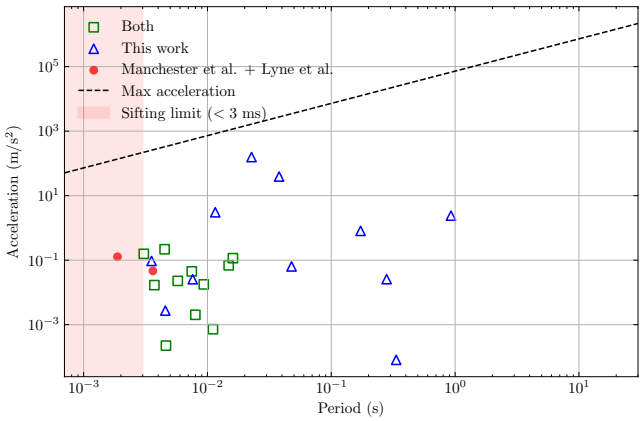

Figure 4. The maximum expected acceleration during the course of the binary orbit is plotted for the set of binary pulsars that were detected. The dashed line indicates the acceleration search limit in the reprocessing for which full sensitivity to accelerated signals was maintained. This limit increases linearly with spin period. The shaded region at periods below $P = 3$ ms indicates where our processing was not sensitive owing to our candidate sifting and removal. The many isolated pulsars detected in the survey (with no measured acceleration in the ATNF pulsar catalog; R. N. Manchester et al. 2005) are not plotted. The original survey processing did not employ an acceleration search, and the 13 accelerated pulsars detected in that search are plotted as green triangles (11) and red circles (2). A significant number (11) of additional accelerated pulsars were detected in our reprocessing but were not found in the original survey (blue triangles). We detected almost all of the original detections (11 out of 13) plus a comparable number (11) of new detections not detected in the original search, indicating the importance of this accelerated search. The two pulsars originally detected but missed by us (PSR J0034−0534 and PSR J1911−1114; red circles) have millisecond periods (and one is below our 3 ms sifting limit), which is likely the reason we missed them (see Section 3.2).

pulsars were found in the gridded beams (R. N. Manchester et al. 1996; A. G. Lyne et al. 1998), but our comparison of pulsar positions with the gridded and targeted beams shows coincidences that suggest some were detected in the targeted beams. Furthermore, we did not detect 79 pulsars in the survey beams that were reported in the original survey as shown in Table 4. These pulsars represent ∼27% of the original detections and some were detected in the remaining targeted beams instead. Since our reprocessing should be at least as sensitive as the original survey, we speculate that these targeted beams were actually part of the original survey coverage. Thus, we compare our results from the reprocessing of both the gridded survey beams and the extra beams with the original results.

3.1. Additional Pulsars Detected in the Survey Reprocessing

Of these 359 pulsars we detected, the original survey did not detect 94 of them. One reason for some of these additional detections is the use of our acceleration search up to $z_{\max} = 50$. Figure 4 shows the maximum expected acceleration during the course of an orbit (derived from the orbital parameters) as a function of spin period for highly accelerated pulsars (binaries with low maximum accelerations, below 10^{-4} m s^{-2}, are not included).

To gauge the detectability of accelerated pulsars in a nonaccelerated search, we did a quick test with the 22 binary pulsars shown in Figure 4. We compared the strength of the signal in the power spectrum, where *z*max was 0 and 50. All of the pulsars appeared as candidates in both of these cases when the data were dedispersed at the known pulsar's DM. However, three pulsars had significant signal reductions in the spectrum from *z*max of 0 compared to the one from *z*max of 50 (the sigma value was reduced to 46% for PSR B0021−72E, 84% for PSR J0737−3039A, and 23% for PSR J2051−0827). In other words, these three pulsars exhibited significant acceleration during the observation, whereas the others did not. It is worth noting that PSR J2051−0827 was detected in the original survey despite being highly accelerated. The plotted points in Figure 4 represented maximum possible accelerations (estimated from the orbital parameters), so it is not surprising that the accelerations actually observed were smaller. This suggests that, although the majority of pulsars did not exhibit increased

Table 3
Statistics of Pulsars Detected in Gridded and Targeted Beams

Description	Total	Gridded	Targeted
Pulsars detected in original survey (R. N. Manchester et al. 1996; A. G. Lyne et al. 1998)	298	...	...
Pulsars detected in this reprocessing	359	256	103
Pulsars detected both in reprocessing and by the original survey	265	219	46
Pulsars detected by the original survey only but not in this reprocessing	33	...	...
Pulsars detected in this reprocessing only but not by the original survey	94	37	57

Note. The number of pulsars blindly detected through our reprocessing from both gridded and targeted beams, as well as the total number (i.e., gridded + targeted). Numbers refer to known pulsars only (i.e., not including the new LMC pulsar, PSR J0540−69).

Table 4
Statistics of Pulsars Detected in the Original PKS70 Survey and this Reprocessing

Description	Number of Beams	Both	$PKS70_{New}$	$PKS70_{Orig.}$
Gridded survey beams	41,342	219	37	33
Targeted (confirmation) beams	1774	46	57	0
Total	43,116	265	94	33

Note. Numbers do not include the new LMC pulsar we discovered in the reprocessing, PSR J0540−69. $PKS70_{New}$ and $PKS70_{Orig.}$ are the number of pulsars detected only by this work and the original survey (R. N. Manchester et al. 1996; A. G. Lyne et al. 1998), respectively. The number of pulsars detected by both works is shown under "Both."

detectability from the acceleration search, at least some would have had better detectability; thus, it was an important parameter space to search, given the availability of computational resources.

We also detected five high-DM pulsars that exceed the maximum DM searched in the original survey. The excess DM for all five pulsars is due to their local environments: four in the SMC or LMC and one in a known supernova remnant, as shown in the left panel of Figure 2. Furthermore, we detected several high-DM pulsars near the Galactic center that the original survey did not detect; the original survey only detected pulsars up to $\sim$550 pc cm^{-3} despite their maximum DM limit of $\sim$777 pc cm^{-3}, whereas we detected several beyond what the original survey detected (see the right panel of Figure 2). The reason for this difference at these large DMs is still uncertain. We found that it is not related to the DM step size used, pulse profile morphology, or observation integrations. One possible reason is that a linear dedispersion approximation was used in the initial subbanding stage in the original processing, which could have resulted in larger DM smearing effects. However, answering this question fully would require more testing and comparison of the approximated dedispersion with the PRESTO dedispersion, which could be addressed in future work.

Finally, the population of pulsars that we detected extends to lower luminosities than those detected in the original survey. We detected 11 pulsars below the nominal survey sensitivity threshold (see Figure 3), but these detections are all from gridded beams with longer integrations.

3.2. Missed Pulsars in the Survey Reprocessing

Despite searching targeted beams in addition to survey beams, we missed 33 pulsars that were detected in the original survey. These are listed in Table 5 along with their refolding status using cataloged parameters and the proposed reason for nondetection (also discussed below).

Of these 33 pulsars, we found that 14 of them have no nearby archival beams within 1 beam size. By cross-checking the position of these 14 pulsars, the available beam positions, and the original survey pointing map (R. N. Manchester et al. 1996),[8] we found that all of them are possibly located next to a missing beam (listed as "missing beams" in the table).

We folded the remaining 19 pulsars with PRESTO (S. Ransom 2011) using their nearby observations within 1 beam size and parameters listed in the ATNF pulsar catalog (R. N. Manchester et al. 2005),[9] and we did not detect 7 of them (listed as "no detection after folding" in the table). This could be due to (a) a different RFI mitigation method/configuration in the processing or (b) the original survey revisited these pointings and detected these pulsars, but the revisited observation was not archived.

Finally, there are 12 pulsars whose signals are present in our data but were not blindly detected (highlighted in bold in Table 6). Among them, four pulsars had a low-detection S/N, as reported in the original surveys (R. N. Manchester et al. 1996; A. G. Lyne et al. 1998), and two have cataloged 400 MHz flux densities (R. N. Manchester et al. 2005) close to our detection threshold. Additionally, 7 of these pulsars are located near the edge of the beam (this includes the pulsars whose closest beam is missing but can still be detected on the edge of another nearby beam). Lastly, there are four MSPs, of which three have poor sensitivity and one has a period $<$3 ms, which was a range that was ignored in the candidate sifting process.

Despite further investigation of potential common properties among those pulsars (e.g., fast rotation or high DM), we did not find any; these pulsars span a wide range of parameter space, as shown in Table 6. Hence, their nondetections are most likely due to our sifting process, which removed candidates that appear in fewer than 10 DM trials. This filters out pulsars with a detection S/N that is too faint to be detected in 10 DM trials. The same is true for MSPs, whose signal can easily become smeared if they have narrow duty cycles, even if they are largely above the nominal detection threshold.

Despite the missing pulsars, the overall larger number of pulsar detections in this reprocessing (359) compared to the original survey (298) generally reinforces the idea that motivated this reprocessing, which is that multiple searches of pulsar data sets are worthwhile, since one search package

[8] We reconstructed the pointing map using the procedure described by R. N. Manchester et al. (1996).
[9] We used PSRCAT version 2.5.1 for the catalog data, and the same version was used consistently throughout the rest of the paper.

Table 5
33 Pulsars Detected in the Original Processing but Not in the Reprocessing

PSR	Refolding Status	Notes and Reason for Nondetection
J0034-0534	**Detected**	**MSP**
J0211-8159	No nearby beams	Missing beams
J0540-7125	No detection	No detection after folding
B0621-04	No detection	No detection after folding
B0903-42	No nearby beams	Missing beams
B0950-38	No nearby beams	Missing beams
B1016-16	No nearby beams	Missing beams
J1024-0719	**Detected**	**Flux density near survey threshold, MSP**
B1105-59	No detection	No detection after folding
J1126-6942	**Detected**	**Missing the closest pointing but detected on another nearby beam**
J1159-7910	**Detected**	**Original survey detection S/N near survey threshold**
B1254-10	No nearby beams	Missing beams
B1309-12	**Detected**	**Flux density near survey threshold, located near edge of the closest beam, original survey detection S/N near survey threshold**
J1332-3032	**Detected**	**Missing the closest pointing but detected on another nearby beam**
J1403-7646	No detection	No detection after folding
B1454-51	No detection	No detection after folding
B1600-27	**Detected**	**Located near edge of the closest beam**
B1630-59	No nearby beams	Missing beams
B1657-13	No nearby beams	Missing beams
B1706-16	No detection	No detection after folding
B1717-29	No nearby beams	Missing beams
B1732-07	No nearby beams	Missing beams
B1737-30	**Detected**	**Located near edge of the closest beam, original survey detection S/N near survey threshold**
B1738-08	**Detected**	**Missing the closest pointing but detected on another nearby beam**
B1740-13	No nearby beams	Missing beams
J1744-1134	**Detected**	**MSP**
B1828-60	No nearby beams	Missing beams
B1841-04	No detection	No detection after folding
B1844-04	No nearby beams	Missing beams
J1911-1114	**Detected**	**MSP, located near edge of the closest beam**
B1940-12	No nearby beams	Missing beams
J1940-2403	**Detected**	**Original survey detection S/N near survey threshold**
B2043-04	No nearby beams	Missing beams

Note. A total of 33 pulsars are on this list. The "refolding status" indicates whether the pulsar was detected by folding on the nearby beams with known parameters obtained from the ATNF pulsar catalog (R. N. Manchester et al. 2005). Pulsars for which signals were presented in our data but were not blindly detected in the search (i.e., detected by refolding) are indicated in bold text.

Table 6
Parameters for 12 Pulsars Missed in a Blind Search but Detected by Refolding

PSR	P (ms)	$\dot{P}$ (s/s)	DM (pc cm^{-3})	S_{400} (mJy)	PKS70$_{\rm orig}$ S/N	Reference for P, $\dot{P}$, DM, and S_{400}
J0034−0534	1.88	4.97×10^{-21}	13.8	24	16	1 2, 3
J1024−0719	5.16	1.85×10^{-20}	6.5	4.6	12	4, 5
J1126−6942	579.42	3.29×10^{-15}	55.3	9	17	6, 7
J1159−7910	525.08	2.81×10^{-15}	59.3	6	10	6, 9
B1309−12	447.52	1.51×10^{-16}	36.2	4.0	8.4	9, 10, 11
J1332−3032	650.43	5.60×10^{-16}	15.1	9	13	6, 12
B1600−27	778.32	3.01×10^{-15}	46.0	20.0	24.5	9, 11, 13
B1737−30	607.07	4.66×10^{-13}	151.9	24.6	9	9 11, 14
B1738−08	2043.09	2.27×10^{-15}	75.3	29	16.5	9, 11, 13
J1744−1134	4.07	8.93×10^{-21}	3.1	18	22	4, 5, 15
J1911−1114	3.63	1.40×10^{-20}	31.0	15	13	3, 16, 17, 18
J1940−2403	1855.23	⋯	63.3	⋯	9	6 8

Note. P, $\dot{P}$, DM, and S_{400} were taken from the ATNF pulsar catalog (R. N. Manchester et al. 2005), and their references are indicated in the last column. PKS70$_{\rm orig}$ S/N is the detection S/N reported in the original PKS70 survey (R. N. Manchester et al. 1996; A. G. Lyne et al. 1998).

References. (1) M. Bailes et al. (1994); (2) A. A. Abdo et al. (2010); (3) I. H. Stairs et al. (1999); (4) M. Bailes et al. (1997); (5) EPTA Collaboration et al. (2023); (6) A. G. Lyne et al. (1998); (7) M. E. Lower et al. (2020); (8) N. D'Amico et al. (1998); (9) M. J. Keith et al. (2024); (10) R. J. Dewey et al. (1985); (11) D. R. Lorimer et al. (1995); (12) G. Hobbs et al. (2004); (13) R. N. Manchester et al. (1978); (14) T. R. Clifton & A. G. Lyne (1986); (15) M. Toscano et al. (1998); (16) D. R. Lorimer et al. (1996); (17) G. Desvignes et al. (2016); (18) R. Spiewak et al. (2022).

Table 7
Survey Archive Detections of the New LMC Pulsar PSR J0540−69

Obs Freq. (MHz)	Observation MJD	Integration Time (hr)	Spin Period (ms)	DM (pc cm^{-3})	S/N	S_{436} (mJy)
436	48633.4	2.8	908.9976(9)	78.8	11.6	0.54
	48634.4	2.8	908.9976(9)	76.4	15.3	0.72
	48743.2	5.0	908.9964(4)	84.2	12.5	0.44
1368	58470.4	7.6	909.0003(5)	52.7	13.3	⋯

Note. The S/N was taken from the reported prepfold sigma in the prepfold plot. The 436 MHz flux density was estimated from the S/N and integration time (see Section 3.3). The formal uncertainty from the fold in the last digit of the period is indicated by the figure in the parentheses. In all cases, the best-fit period derivative in the detection was consistent with zero. All three beams were centered on the position of PSR B0540−69. Folded profile detections are shown in Figure 5.

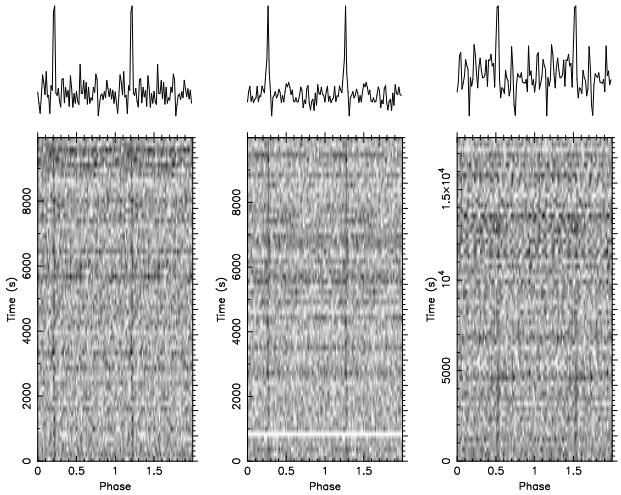

Figure 5. Folded profile detections of three detections of the new LMC pulsar PSR J0540−69, which was discovered in observations targeting PSR B0540−69 (see Table 7). Each subplot shows pulse phase on the horizontal axis (repeated twice for visual clarity) and time subintegrations on the vertical axis. The summed profile is shown at the top of each subplot. The two rightmost plots show some possible variability over the course of the integration, which produces a range of flux density estimates shown in Table 7 that were obtained from the folded S/N values.

(with a particular set of search parameters and capabilities) may miss a pulsar while another may detect it (e.g., M. J. Keith et al. 2009; R. P. Eatough et al. 2013; B. Knispel et al. 2013, 2015; V. Morello et al. 2019; R. Sengar et al. 2023, 2025).

3.3. A New LMC Pulsar, PSR J0540−69

During the reprocessing, we discovered one new pulsar in three long targeted observations of the X-ray pulsar PSR B0540−69 that were part of the survey archive. This pulsar, PSR J0540−69, has a spin period of 0.909 s and a DM of 80 pc cm^{-3} (see Table 7). This DM indicates it is located in the LMC, given the range of DMs observed for LMC pulsars and the expected maximum Galactic DM along the line of sight of 50–60 pc cm^{-3} (J. M. Cordes & T. J. W. Lazio 2002; J. M. Yao et al. 2017). Folded profile detections are shown in Figure 5. Its DM and period indicate that PSR J0540−69 is not associated with PSR B0540−69, the original target of each of these observations, and that it is a new discovery.

A search of two additional PKS70 beams from the archive that covered the position did not show the pulsar. One of these nondetections was from a 10 hr integration at 600 MHz. We subsequently downloaded every other beam available in the

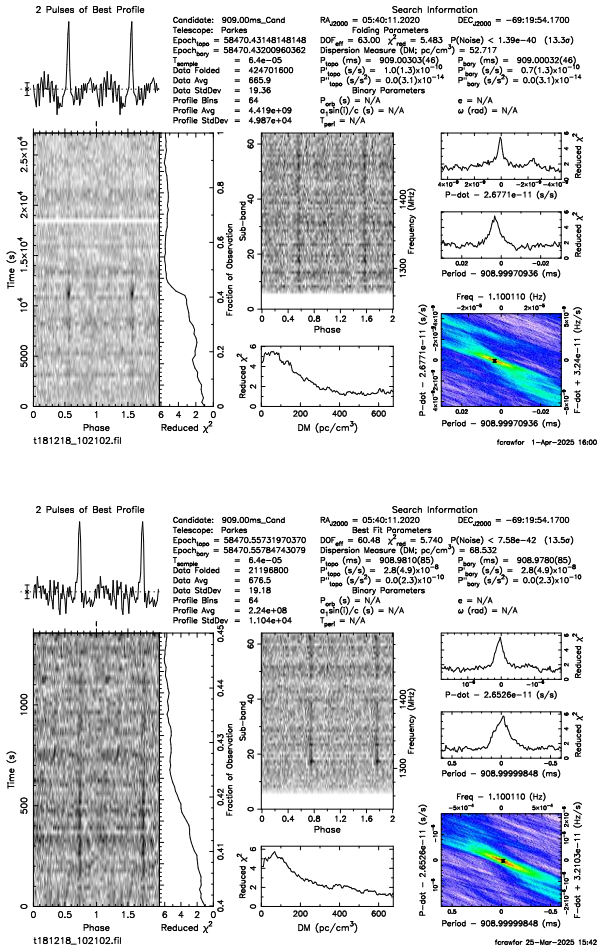

Figure 6. (Top) Detection of J0540−69 in a 1400 MHz 7.6 hr Parkes observation obtained from the CSIRO archive. This was the only other detection (apart from the three PKS70 detections) out of 47 archived observations that overlapped the beam area of the original PKS70 detections. The pulsar exhibits high variability on a timescale of tens of minutes, and therefore, no accurate flux density estimate is possible from this detection. (Bottom) A fold of the 5% of the integration where the pulsar was brightest. The S/N is about the same as in the top fold. There is an indication of variability across the band in this subintegration on a 100 MHz scale, unlike the full fold, in which no variability is indicated. The best-fit DM is somewhat lower than the DM found on the 436 MHz detections, but it is not well localized in this observation (see Figure 7).

CSIRO archive that pointed within 20′ of PSR 0540−69; this is the half power beamwidth of the PKS70 survey beams, and our detections constrained the new pulsar position to within this radius. Each of these beams was dedispersed and folded at DMs and periods near the discovery values. Of the 45

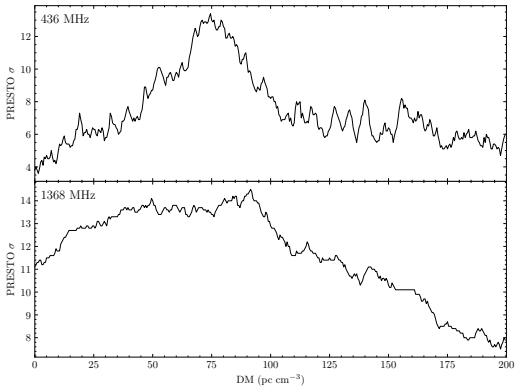

Figure 7. Signal strength (from the sigma value in prepfold) vs. trial DM for folds of PSR J0540−69 at the discovery periods. The top and bottom plots show folds at a range of DM trials for both the 436 and 1380 MHz observations, respectively. The DM is more well localized at 436 MHz (but the DM cannot be constrained better than about 5 or 10 pc cm^{-3} or so), while the DM at the 1368 MHz DM is not well localized. This is accounted for by the higher frequency and less of a smearing effect when folding at an offset DM (especially since the intrinsic pulse width in the fold is relatively wide given its 909 ms period).

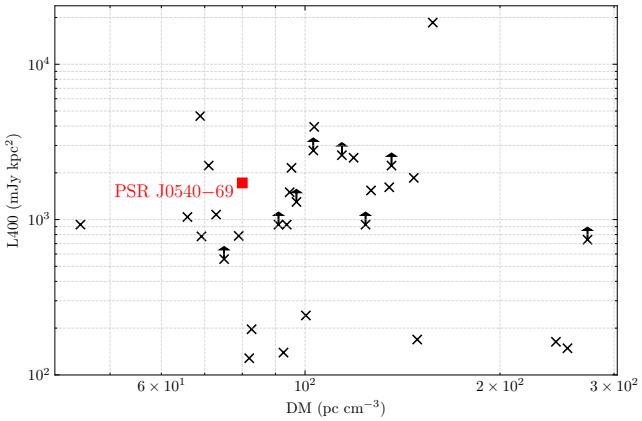

Figure 8. Estimated 400 MHz luminosity vs. DM for the 31 currently known radio pulsars in the LMC (black crosses) and the new pulsar PSR J0540−69 reported here (red square). This includes the 24 pulsars currently listed in the ATNF pulsar catalog (but not PSR J0537−6910 since it is not observed to be a radio emitter) as well as 7 new discoveries reported in the LMC by V. Prayag et al. (2024) in the lower part of the plot. In all, 2 pulsars (PSRs B0456−69 and B0502−66) have cataloged 400 MHz radio luminosities, while the remainder have 1400 MHz values that were scaled to 400 MHz, assuming a spectral index of −1.6 (F. Jankowski et al. 2018). The 1400 MHz flux densities (or lower limits, indicated by arrows in several cases) were taken from the ATNF pulsar catalog (R. N. Manchester et al. 2005) and from Tables 1 and 4 of V. Prayag et al. (2024).

observations searched (excluding the two PKS70 nondetections mentioned above), only one revealed a detection. This detection was in a 1368 MHz beam that targeted PSR B0540−69 for 7.6 hr and is shown in Figure 6. This further constrains the position of PSR J0540−69 to within 7′ of PSR B0540−69 given this is the Parkes beam radius at this frequency.

As seen in Figure 6, the pulsar's brightness varies greatly in time over this 7.6 hr integration on a timescale of tens of minutes. The central part of the observation is where the pulsar is brightest: folding just the brightest 5% of the data (1360 s, or 23 minutes) shows a detection almost as strong as the fold of the full integration. Note that the variability is not noticeable across the 256 MHz bandwidth in the full integration. Folding just the brightest 5% of the integration does show some possible flux variability across the bandwidth, with a scale of order 100 MHz, which is also shown in the frequency panel of Figure 6. The fact that the pulsar appeared in some *L*-band beams but not in most of them illustrates the highly variable nature of this pulsar. This is reinforced by the variability seen in the single 1368 MHz detection. Note that the DM is also less constrained and appeared to be lower in this L-band detection than in 436 MHz detections, in part due to less smearing at higher frequencies, as shown in Figure 7.

PSR J0540−69 has also not been detected in the recent high-resolution TRAMPUM LMC survey (V. Prayag et al. 2024). By retrieving the beam positions from the MeerKAT SARAO archive[10] and matching them with the detection position of PSR J0540−69, it can be seen that the pulsar was covered by the TRAMPUM survey region but at the edge of the nearest beam. Owing to this, and its high variability, PSR J0540−69 may not be present in the MeerKAT observations.

Integrated pulse profiles at both 436 and 1368 MHz show a single-pulse component of moderate width (6% of the pulse period), suggesting that there is no profile evolution between these frequencies.

We used the 1368 MHz detection to estimate a rough period derivative for the pulsar by comparing the period of the first 436 MHz detection with the (much later) 1368 MHz detection. This period derivative was about 3×10^{-15}, with a nominal uncertainty of about 30% in this value, as obtained from the uncertainties in the fitted periods. This value is typical for long-period pulsars, suggesting that this pulsar is not remarkable compared to the observed pulsar population.

The variability in the 1368 MHz detection (and the 22 other nondetections in observations taken at or near this frequency) precludes an accurate estimate of the flux density at 1400 MHz. Thus, we cannot reliably estimate a radio spectral index for PSR J0540−69 from these observations. This is not the case at 436 MHz, where the detections are less variable on the timescale of the integrations. We can therefore estimate the flux density at this frequency.

Given the detection at 1368 MHz and its constraint on the position of the pulsar, we can reasonably assume that the pulsar is located near the beam center (within 7′) relative to the PKS70 20′ beam radius. Thus, we would not expect significant attenuation in the PKS70 detections from a beam offset position.

Using the quoted flux density limit at high Galactic latitudes of 3 mJy from the original survey (R. N. Manchester et al. 1996) for a S/N threshold of 8, we scale the sensitivity to account for several factors: the different integration times, the different pulsed duty cycle (6% measured for PSR J0540−69 versus 8% assumed for the survey average), the S/N of the detections, and the different sky temperature at the observed location of PSR J0540−69. For this last point, the original paper (R. N. Manchester et al. 1996) indicated a receiver temperature of 50 K and a sky temperature of 25 K (away from the Gal plane), giving a system temperature of 75 K.

The C. G. T. Haslam et al. (1982) sky temperature map gives a sky temperature of 37 K at 436 MHz at the position of PSR J0540−69, which gives a system temperature of 87 K.

[10] https://archive.sarao.ac.za/

This ratio of system temperatures represents a decrease in sensitivity by a factor of 1.16 for the J0540−69 observations relative to that assumed for the survey. However, the measured, narrow pulsed duty cycle of 6%, compared to the 8% assumed in the survey sensitivity calculation, yields an increase in sensitivity of 1.17, which almost exactly cancels out the effect of the larger system temperature. This leaves the scaling of S/N and integration time factors as the two main contributing factors in determining the flux density.

From this scaling, we obtained flux density values of between 0.4 and 0.7 mJy (see Table 7). We use 0.6 mJy as a reasonable estimate based on these values.

3.4. Comparison with Other LMC Radio Pulsars

Figure 8 shows the estimated 400 MHz luminosity versus DM for the known radio pulsar population in the LMC as well as the PSR J0540−69. To estimate the 400 MHz luminosity for PSR J0540−69, we used the estimated flux density of 0.6 mJy at 436 MHz (see above) and scaled it to 400 MHz using an assumed spectral index of −1.6, which is representative of the known pulsar population (F. Jankowski et al. 2018; giving 0.69 mJy, an almost 15% increase). For a 50 kpc distance from the LMC (G. Pietrzyński et al. 2013), this gives a 400 MHz luminosity of 1725 mJy kpc^2. The 400 MHz luminosity values for the rest of the known LMC pulsars were obtained in all but two cases[11] by scaling the cataloged 1400 MHz values using an assumed spectral index of −1.6 (see above). The ATNF catalog records 24 LMC pulsars (excluding PSR J0537−6990, which is not a radio emitter), while seven new LMC pulsar discoveries were recently reported by V. Prayag et al. (2024), resulting in 31 pulsars, plus the radio pulsar we report here. According to Figure 8, J0540−69 has an estimated DM and radio luminosity that is in the range of other LMC pulsars.

4. Conclusions

We have presented the results of the reprocessing of the archived PKS70 survey using PRESTO. We searched an extended DM range and performed an acceleration search on all of the archival data. We detected 359 known pulsars, of which 265 were detected in the original survey and 94 were not but could in principle have been detected at that time. Among these 94 known pulsars, we also detected several highly accelerated pulsars that may have been missed in the original survey due to the absence of an acceleration search. We missed 33 (of the 298) pulsars that were originally detected in the survey, due in part to portions of the survey data that are missing from the survey archive and our early-stage candidate sifting method.

We have also discovered a new LMC pulsar, PSR J0540−69, in three archival PKS70 436 MHz survey beams that targeted PSR B0540−69 in the LMC. PSR J0540−69 has a spin period of 0.909 s and a DM of 80 pc cm^{-3}. The pulsar's DM suggests that it resides in the LMC. In addition to PKS70 observations, one further detection of the pulsar was made at 1368 MHz in an archival observation of PSR B0540−69. This detection revealed significant flux variability on a timescale of tens of minutes. This may account for why it was not seen in other archival beams targeting PSR B0540−69. We do not have timing information to allow for further investigation of its properties and localization beyond the 1368 MHz beam size, but the difference in spin periods at the different epochs suggests that its spin-down rate is not unusual. Planned future work with this data set includes conducting a search for long-period pulsars using the FFA algorithm (e.g., V. Morello et al. 2020).

[11] PSRs B0456−69 and B0502−66 already have cataloged 400 MHz luminosities (R. N. Manchester et al. 2005).

Acknowledgments

We thank the students at the following institutions for their assistance with classifying pulsar candidates using the candidate viewer: Franklin and Marshall College, Kumamoto University, Hillsdale College, Kenyon College, the University of Puerto Rico at Mayagüez, Reed College, Vanderbilt University, Oregon State University, and the University of Wisconsin-Milwaukee. We also thank the anonymous referee for the insightful and helpful comments that helped improve the final manuscript. Murriyang, CSIRO's Parkes radio telescope, is part of the Australia Telescope National Facility (https://ror.org/05qajvd42), which is funded by the Australian Government for operation as a National Facility managed by CSIRO. This paper includes archived data obtained through the Parkes Pulsar Data archive on the CSIRO Data Access Portal (http://data.csiro.au). This work was supported in part by the National Science Foundation (NSF) Physics Frontiers Center award Nos. 1430284 and 2020265 and used the Franklin and Marshall College compute cluster, which was funded through NSF grant 1925192.

ORCID iDs

Wenke Xia https://orcid.org/0009-0009-9343-4193
Fronefield Crawford https://orcid.org/0000-0002-2578-0360
Shinnosuke Hisano https://orcid.org/0000-0002-7700-3379

References

Abdo, A. A., Ackermann, M., Ajello, M., et al. 2010, ApJ, 712, 957
Bailes, M., Harrison, P. A., Lorimer, D. R., et al. 1994, ApJL, 425, L41
Bailes, M., Johnston, S., Bell, J. F., et al. 1997, ApJ, 481, 386
Cameron, A. D., Champion, D. J., Kramer, M., et al. 2018, MNRAS, 475, L57
Clifton, T. R., & Lyne, A. G. 1986, Natur, 320, 43
Cordes, J. M., & Lazio, T. J. W. 2002, arXiv:astro-ph/0207156
Crawford, F., Hisano, S., Golden, M., et al. 2022, MNRAS, 515, 3698
D'Amico, N., Stappers, B. W., Bailes, M., et al. 1998, MNRAS, 297, 28
Desvignes, G., Caballero, R. N., Lentati, L., et al. 2016, MNRAS, 458, 3341
Dewey, R. J., Taylor, J. H., Weisberg, J. M., & Stokes, G. H. 1985, ApJL, 294, L25
Eatough, R. P., Kramer, M., Lyne, A. G., & Keith, M. J. 2013, MNRAS, 431, 292
EPTA Collaboration, Antoniadis, J., Babak, S., et al. 2023, A&A, 678, A48
Haslam, C. G. T., Salter, C. J., Stoffel, H., & Wilson, W. E. 1982, A&AS, 47, 1
Hobbs, G., Lyne, A. G., Kramer, M., Martin, C. E., & Jordan, C. 2004, MNRAS, 353, 1311
Jankowski, F., van Straten, W., Keane, E. F., et al. 2018, MNRAS, 473, 4436
Kaplan, D. L. 2022, Pulsar Survey Scraper, Astrophysics Source Code Library, ascl:2210.001
Keith, M. J., Eatough, R. P., Lyne, A. G., et al. 2009, MNRAS, 395, 837
Keith, M. J., Johnston, S., Karastergiou, A., et al. 2024, MNRAS, 530, 1581
Knispel, B., Eatough, R. P., Kim, H., et al. 2013, ApJ, 774, 93
Knispel, B., Lyne, A. G., Stappers, B. W., et al. 2015, ApJ, 806, 140
Lorimer, D. R., Lyne, A. G., Bailes, M., et al. 1996, MNRAS, 283, 1383
Lorimer, D. R., Yates, J. A., Lyne, A. G., & Gould, D. M. 1995, MNRAS, 273, 411
Lower, M. E., Bailes, M., Shannon, R. M., et al. 2020, MNRAS, 494, 228
Lyne, A. G., Manchester, R. N., Lorimer, D. R., et al. 1998, MNRAS, 295, 743

Manchester, R. N., Hobbs, G. B., Teoh, A., & Hobbs, M. 2005, AJ, 129, 1993
Manchester, R. N., Lyne, A. G., D'Amico, N., et al. 1996, MNRAS, 279, 1235
Manchester, R. N., Lyne, A. G., Taylor, J. H., et al. 1978, MNRAS, 185, 409
Morello, V., Barr, E. D., Cooper, S., et al. 2019, MNRAS, 483, 3673
Morello, V., Barr, E. D., Stappers, B. W., Keane, E. F., & Lyne, A. G. 2020, MNRAS, 497, 4654
Pietrzyński, G., Graczyk, D., Gieren, W., et al. 2013, Natur, 495, 76
Prayag, V., Levin, L., Geyer, M., et al. 2024, MNRAS, 533, 2570
Ransom, S., 2011 PRESTO: PulsaR Exploration and Search TOolkit, Astrophysics Source Code Library, ascl:1107.017
Ransom, S. M. 2001, PhD thesis, Harvard Univ., Massachusetts
Ransom, S. M., Eikenberry, S. S., & Middleditch, J. 2002, AJ, 124, 1788
Sengar, R., Bailes, M., Balakrishnan, V., et al. 2023, MNRAS, 522, 1071
Sengar, R., Bailes, M., Balakrishnan, V., et al. 2025, MNRAS, 536, 3159
Seward, F. D., Harnden, F. R., Jr., & Helfand, D. J. 1984, ApJL, 287, L19
Spiewak, R., Bailes, M., Miles, M. T., et al. 2022, PASA, 39, e027
Stairs, I. H., Thorsett, S. E., & Camilo, F. 1999, ApJS, 123, 627
Taylor, J. H. 1974, A&AS, 15, 367
Taylor, J. H., & Weisberg, J. M. 1989, ApJ, 345, 434
Toscano, M., Bailes, M., Manchester, R., & Sandhu, J. 1998, ApJ, 506, 863
Weisberg, J. M., & Taylor, J. H. 2003, in ASP Conf. Ser. 302, Radio Pulsars, ed. M. Bailes, D. J. Nice, & S. E. Thorsett (San Francisco, CA: ASP), 93
Weisberg, J. M., & Taylor, J. H. 2005, in ASP Conf. Ser. 328, Binary Radio Pulsars, ed. F. A. Rasio & I. H. Stairs (San Francisco, CA: ASP), 25
Yao, J. M., Manchester, R. N., & Wang, N. 2017, ApJ, 835, 29